# Jahn-Teller effects in the $C_{60}^{2+}$ cation undergoing $D_{2h}$ distortion

Ian D. Hands, Wajood A. Diery,* Colin A. Bates,† and Janette L. Dunn‡
*School of Physics and Astronomy, University of Nottingham, University Park, Nottingham, NG7 2RD, United Kingdom*
(Received 8 March 2007; revised manuscript received 8 May 2007; published 20 August 2007)

It has recently been shown that the high-spin, doubly hole-doped fullerene cation $C_{60}^{2+}$ is likely to undergo a Jahn-Teller (JT) distortion, which reduces the molecular symmetry from $I_h$ to $D_{2h}$. A theoretical model for the JT effect describing this situation is presented. The model includes parameters for the energy differences between molecular terms that arise from Coulomb interactions between the holes. Although the magnitudes of these parameters are not known to any degree of certainty for the $C_{60}^{2+}$ cation, they are likely to have an important effect. Results are given for both the static JT effect, where the motion of the system can be considered in terms of vibrations in a potential well, and the dynamic JT effect, where tunneling between equivalent wells must be taken into account.

DOI: 10.1103/PhysRevB.76.085426 PACS number(s): 61.48.+c, 31.30.Gs, 33.20.Wr

## I. INTRODUCTION

Although difficult to prepare in the laboratory, hole-doped fullerenes are expected to have exceptional properties that make them even more alluring than their negatively doped counterparts. For example, calculations by Manini *et al.*[1] indicate that the electron-phonon coupling in positively charged fullerene derivatives $C_{60}^{n+}$ is significantly larger than in the corresponding negatively charged ions $C_{60}^{n-}$. Alternative calculations also allow the deduction that the electron-phonon coupling is stronger in $C_{60}^{+}$ than it is in $C_{60}^{-}$.[2] In addition, interpretation of experimental measurements also indicate that the coupling is strong in $C_{60}^{+}$.[3] Thus we can expect that there may be hole-doped fullerene derivatives that exhibit critical temperatures for superconductivity that exceed even those found in the electron-doped fullerides. However, the electron-phonon coupling is in direct competition with the intramolecular Coulomb exchange interaction. Thus both interactions must be considered simultaneously in any theoretical analysis of these ions. The two interactions can lead to opposite conclusions regarding spin. The electron-phonon interaction tends to promote low-spin ground states, while Coulomb interactions lead to high-spin ground states.[4]

The hole(s) of $H_u$ symmetry in $C_{60}^{n+}$ cations can couple to two $a_g$, six $g_g$, and eight $h_g$ modes of vibration. However, it has been shown that the $a_g$ and $g_g$ modes do not result in any significant couplings.[1] Also, coupling to one of the $h_g$ modes [namely $h_g(1)$] is believed to be much stronger than the couplings to the other modes.[1] Therefore the electron-phonon coupling may be described, in the first instance, in terms of coupling to a single $h_g$ mode only. If it is found desirable to consider the couplings to all eight $h_g$ modes, then it is possible to formulate the problem in terms of a single effective mode[5] and so the system can still be treated in terms of a single $h_g$ mode but with different numerical values for the constants than those for the $h_g(1)$ mode alone.

In the singly doped cation $C_{60}^{+}$, the complication presented by Coulomb interactions are absent, and so the model involves Jahn-Teller (JT) interactions only. The system can be represented by a $H_u \otimes h_g$ JT problem, which results in wells in the lowest adiabatic potential energy surface (APES) having either $D_{5d}$ or $D_{3d}$ symmetry,[6–8] in common with results for the negatively charged fullerene ions. Multiply hole-doped molecules $C_{60}^{n+}$ can be similarly described using, in the notation of Nikolaev *et al.*,[9] a $(h_u^+)^n \otimes h_g$ JT coupling model. In these cases, Coulomb interactions are important and must be given due consideration alongside the JT effects. It is found that these ions may have distortions that are of $D_{2h}$ or $C_{2h}$ symmetry, in addition to the more usual $D_{5d}$ and $D_{3d}$ ones.[10,11]

In the present paper, we concentrate on the doubly hole-doped cation $C_{60}^{2+}$, which we model as a linear $(h_u^+)^2 \otimes h_g$ JT system. In systems with wells in the APES, such as is the case here, the effect of higher-order couplings is only to introduce small changes to the positions and depths of the wells, so can be safely neglected. (This is in contrast to cases where the APES contains a trough of accidentally higher symmetry, in which case higher-order terms will warp the trough and potentially convert rotational motion into vibrations.) Furthermore, numerical values for the linear constants are still not known to any degree of accuracy for the $C_{60}^{n+}$ ions, and values for higher-order constants are not known at all. Hence adding higher-order terms would only introduce additional unknown parameters into an already complicated system.

There are several additional complications that arise in this system. First, the two holes may couple to produce terms having either low ($S=0$) or high ($S=1$) spin. Calculations indicate that the high-spin terms are the lower in energy,[9] and so we shall henceforth ignore the low-spin terms. The high-spin terms are $\{^3T_{1g}, ^3T_{2g}, ^3G_g\}$, which means that the JT effect must be formulated using a ten-dimensional electronic basis. Second, the three terms used in the basis do not have the same energy because of the Coulomb interaction between the two holes from which the multihole states of the system can be derived. The terms will have different energies, irrespective of any JT interactions. Calculations of the Coulomb term energies for the $C_{60}^{2+}$ ion appearing in the literature are not in agreement with each other.[4,9,12,13] Thus it is not currently possible to give an unequivocal treatment of the ion. However, we can develop a model in which the term splittings are treated as parameters, and calculate results for various values of those parameters.

 

A third complication lies in the nonsimple reducibility of the product $H \otimes h$ within the icosahedral symmetry group which means that there are two sets of Clebsch-Gordan (CG) coefficients required to describe the interaction which are not symmetry related.[14] The symmetry of any JT distortion depends intimately on the precise combination of coefficients used.[15] Theoretically, the general $(h_u^+)^2 \otimes h_g$ JT system can be distorted into $D_{5d}$, $D_{3d}$, $D_{2h}$ or $C_{2h}$ symmetry.[15]

Yet another complication is that the $C_{60}^{2+}$ ion has eight $h_g$ modes of vibration that all contribute to the vibronic coupling problem. As each mode must be described by two (linear) coupling constants, this means that 16 linear coupling constants are needed in total to provide a complete description of linear coupling in the $C_{60}^{2+}$ ion. If quadratic or other higher-order couplings are included, the number of parameters needed is even higher. However, calculated values of the linear coupling constants[1,16] suggest that the $h_g(1)$ mode is much more strongly coupled than the others, and therefore dominates the distortion. The overall effect of this dominance is to favor a $D_{2h}$ distortion of the ion as a whole.[10,15] It therefore seems reasonable to consider the vibronic coupling problem for $C_{60}^{2+}$ in terms of a single mode favoring $D_{2h}$ distortions, which is what we will do in this paper. Although quadratic and other higher-order terms could be important, we will not consider them in this paper as they are not likely to have a large effect on our overall results.

A detailed consideration of the general $(h_u^+)^2 \otimes h_g$ JT system has recently been given.[17] In that paper, all four of the possible symmetry distortions mentioned above were considered, but the Coulomb term splittings were not taken into account. In this paper, we will reconsider the $D_{2h}$ case and take the Coulomb splittings into account. This extends preliminary results obtained for $D_{2h}$ wells in the absence of term splittings.[19]

In Sec. II, details are given of the derivation of the interaction Hamiltonian for the $C_{60}^{2+}$ ion, and an analysis of the lowest APES associated with the Hamiltonian is given in Sec. III, assuming that $D_{2h}$ distortions prevail. Further details on the 15 well states associated with the $D_{2h}$ minima are given in Sec. IV. These states are good states for the system as a whole if the JT coupling is infinitely strong and the system becomes statically distorted into one of the 15 $D_{2h}$ configurations. However, for finite JT coupling, the system can tunnel between the wells giving rise to a dynamic JT effect. This may be accounted for by formulating so-called symmetry-adapted states from the well states to generate vibronic states having the correct symmetry for the problem. Such states, and their energies, are also considered in Sec. IV. Finally, some general conclusions are given in Sec. V.

## II. THE INTERACTION HAMILTONIAN

A good understanding of the properties of the $C_{60}^{2+}$ JT ion can be obtained from an analysis of the properties of the lowest APES. This involves the vibrational and JT potential energy terms and the associated electronic term energies. The high-spin states, which are predicted to be lowest in energy,[9] can be obtained in terms of single-hole states[17,18] from tables of CG coefficients.[14]

The next stage is to derive the interaction Hamiltonian $\mathcal{H}_{int}$ which describes the coupling between the electrons and the vibrations of molecules occupying these spin triplet basis states. As discussed above, there are two sets of CG coefficients involved. We add labels $a$ and $b$ to those parts of the interaction Hamiltonian arising from the CG coefficients given in the first and second columns, respectively, in the tables of CG coefficients given in Ref. 14. Thus

$$\mathcal{H}_{int} = V_{Hh_a}\mathcal{H}_a + V_{Hh_b}\mathcal{H}_b, \tag{1}$$

where $V_{Hh_a}$ is the single-hole coupling constant (i.e., the coupling constant for the $H \otimes h$ JT system) appropriate to the coupling described by the set $a$ of CG coefficients and $\mathcal{H}_a$ is the corresponding interaction Hamiltonian. $V_{Hh_b}$ and $\mathcal{H}_b$ are the similar quantities for set $b$.

Alternatively, we can write the vibronic coupling constants in the polar form

$$V_{Hh_a} = V \sin\beta,$$

$$V_{Hh_b} = V \cos\beta \tag{2}$$

as was done by Manini *et al.*[20] for the $H \otimes h$ JT system. The angle $\beta$ represents a mixing of the two different sets of CG coefficients and $V$ is a measure of the combined coupling strength.

In our calculations, we will include the interactions between the high-spin terms only so that our electronic basis may be written as $\{^3T_{1g}, ^3T_{2g}, ^3G_g\}$ and the JT interaction Hamiltonians, $\mathcal{H}_a$ and $\mathcal{H}_b$, can each be written as $10 \times 10$ matrices. The matrices can be split into block form such that each block represents coupling between certain specified terms. Each block contains a numerical constant involving $V_{Hh_a}$ and $V_{Hh_b}$, or equivalently $V$ and $\beta$,[17] and matrices involving the components $(Q_\theta, Q_\epsilon, Q_x, Q_y, Q_z)$ of the oscillator representing the $h_g$ mode of vibration that follow directly from the tables of Ref. 14.

Now that the interaction Hamiltonian has been formulated, we can begin to analyze the ground state APES associated with the full Hamiltonian,

$$\mathcal{H} = \mathcal{H}_{term} + \mathcal{H}_0 + \mathcal{H}_{int}. \tag{3}$$

$\mathcal{H}_{term}$ represents the contribution from the Coulomb term energies, which we take to be a diagonal matrix with diagonal elements of $(\mathcal{E}_{T_1}, \mathcal{E}_{T_1}, \mathcal{E}_{T_1}, \mathcal{E}_{T_2}, \mathcal{E}_{T_2}, \mathcal{E}_{T_2}, \mathcal{E}_G, \mathcal{E}_G, \mathcal{E}_G, \mathcal{E}_G)$, where $\{\mathcal{E}_{T_1}, \mathcal{E}_{T_2}, \mathcal{E}_G\}$ are the energies of the $T_1$, $T_2$, and $G$ states, respectively, in the limit of zero vibronic coupling,

$$\mathcal{H}_0 = \frac{1}{2}\sum_i \left(\frac{1}{\mu}P_i^2 + \mu\omega^2 Q_i^2\right) I \tag{4}$$

is the Hamiltonian for the system in the absence of vibronic coupling, where the sum $i$ is taken over the five components of the $h_g$ mode and $I$ is the unit $10 \times 10$ matrix. In this expression, $P_i$ is the momentum operator conjugate to $Q_i$, $\mu$ is the reduced mass of the oscillators, and $\omega$ is their frequency.

### III. ANALYSIS OF THE $C_{60}^{2+}$ GROUND APES

In order to focus our attention on the ground vibronic state, we make use of a shift transformation[21,22] using the unitary operator

$$U = \exp\left(\mathrm{i}\sum_j \alpha_j P_j\right), \tag{5}$$

where the parameters $\alpha_j$ are coefficients that may be varied to minimize the energy. The commutator of $U$ and $Q_j$ is simply $[U,Q_j]=\hbar\alpha_j U$, so the transformation has the effect of shifting the $Q_j$ coordinate by an amount equal to $\hbar\alpha_j$. The commutator of $U$ and a general quadratic combination of phonon modes is $[U,Q_jQ_k]=\hbar U(\alpha_jQ_k+\alpha_kQ_j-\hbar\alpha_j\alpha_k)$, and so the transformed Hamiltonian $\tilde{\mathcal{H}}=U^{-1}\mathcal{H}U$ may be split into two terms, $\tilde{\mathcal{H}}^{(1)}$ and $\tilde{\mathcal{H}}^{(2)}$, such that $\tilde{\mathcal{H}}^{(2)}$ contains all terms which have explicit dependence on the phonon operators and $\tilde{\mathcal{H}}^{(1)}$ consists of all the other, phonon independent, terms. The latter Hamiltonian is therefore a good Hamiltonian for determining the ground states of the system.

We can simplify the constants involved in the problem by working with the Hamiltonian

$$\tilde{\mathcal{H}}^{(1)\prime} = \frac{\mu\omega^2}{V^2}\tilde{\mathcal{H}}^{(1)}. \tag{6}$$

If we write

$$V' = -\frac{V}{\sqrt{\mu\hbar\omega^3}},$$

$$\alpha_i = \frac{V}{\hbar\mu\omega^2}a_i,$$

$$\mathcal{H}_{int} = V\mathcal{H}'_{int},$$

$$\mathcal{H}_{term} = V'^2\hbar\omega\mathcal{H}'_{term} \tag{7}$$

it then follows that

$$\tilde{\mathcal{H}}^{(1)\prime} = \mathcal{H}'_{term} + \frac{1}{2}\sum_i a_i^2 I + \mathcal{H}'_{int}(Q_i \mapsto -a_i) \tag{8}$$

[where $\mathcal{H}'_{int}(Q_i\mapsto -a_i)$ indicates $\mathcal{H}'_{int}$ with the $Q_i$ replaced by $-a_i$]. This expression neglects the zero-point energy associated with each oscillator. There are ten eigenvalues of $\tilde{\mathcal{H}}^{(1)\prime}$, which we will call $\{\lambda_1,\ldots,\lambda_{10}\}$ and order according to their numerical values such that the energy of the ground state will be associated with $\lambda_1$. The corresponding electronic state will be associated with the eigenvector which we will call $\boldsymbol{x}_1$. The symmetry of the wells associated with these minimum energies depends on the mixing angle and term splitting.[15] For example, when the term splitting is zero, $\mathcal{H}_a$ alone ($\beta=\pi/2$) results in $C_{2h}$ symmetry, whereas $\mathcal{H}_b$ alone ($\beta=0$) results in $D_{2h}$ symmetry. Combinations of $\mathcal{H}_a$ and $\mathcal{H}_b$ can result in $D_{3d}$ or $D_{5d}$ symmetry.[15,17]

As there are 15 equivalent $D_{2h}$ wells, there must be 15 eigenvectors $\boldsymbol{x}_1$ that produce $D_{2h}$ wells of the same energy at any given mixing angle $\beta$. When the Coulomb term interactions are ignored and when the mixing angle $\beta=0$, one of these states is

$$\boldsymbol{x}_1 = (0,0,\sqrt{3/10},0,0,\sqrt{3/10},0,0,0,\sqrt{2/5}). \tag{9}$$

The energy associated with the well is $-E_{JT}$, where

$$E_{\mathrm{JT}} = \frac{9}{16}V'^2\hbar\omega \equiv \frac{9}{16}\frac{V^2}{\mu\omega^2} \tag{10}$$

is the JT energy.

If we now include the term energies and choose a nonzero mixing angle, then we find, numerically, that the $D_{2h}$ eigenvector that reduces to that in Eq. (9) when $\beta=0$ and the term splittings are zero has the general form

$$\boldsymbol{x}_1 = (0,0,s_1,0,0,s_2,0,0,0,s_3), \tag{11}$$

where $s_1$, $s_2$, and $s_3$ depend on the term energies and $\beta$. For now, we leave the precise form of these quantities undetermined and merely take them to be variables (subject to the normalization condition $s_1^2+s_2^2+s_3^2=1$). We note that the assumption that one of the wells has a general electronic component of the form shown in Eq. (11) is essentially orienting the system so that one $D_{2h}$ well is aligned in the $z$ direction. Our coordinates are such that this direction coincides with a molecular $C_2$ axis which passes through a pair of carbon-carbon double bonds. Thus this $D_{2h}$ well can be thought of as being associated with the uppermost double bond of $C_{60}^{2+}$ as shown in Fig. 1(a), or the lowermost counterpart of this double bond. Similarly, the remaining $D_{2h}$ wells can be associated with the other diametrically opposite pairs of double bonds. The positions of the minima on the icosahedron (i.e., the centers of the double bonds of $C_{60}^{2+}$) can be connected together, forming an icosidodecahedron as shown in Fig. 1(b).

We can view the eigenvector in Eq. (11) as a "generating state." Starting from this eigenvector, we can use the group operations for the $I_h$ point group to obtain the other equivalent wells. The fact that applying these operations to one well state generates one of the other well states also proves that the states do indeed have $D_{2h}$ symmetry. Also, we can use the generating state to determine the shift parameters $\alpha_i$ required in order to minimize the energy associated with each well. Having found expressions for the wells, we can then use projection operators to form symmetry-adapted states from them and, subsequently, find expressions for their energies.

For a general mixing angle, the eigenvalue corresponding to the eigenvector in Eq. (11) is given by

$$\lambda_1 = \boldsymbol{x}_1^{\mathsf{T}}\tilde{\mathcal{H}}^{(1)\prime}\boldsymbol{x}_1. \tag{12}$$

The next step is to minimize $\lambda_1$ with respect to the shifts $\{a_i\}$. That is, we seek shifts such that

$$\frac{\partial\lambda_1}{\partial a_i} = \boldsymbol{x}_1^{\mathsf{T}}\frac{\partial\tilde{\mathcal{H}}^{(1)\prime}}{\partial a_i}\boldsymbol{x}_1 = 0. \tag{13}$$

Using Eq. (8), this condition implies that the minimum occurs when

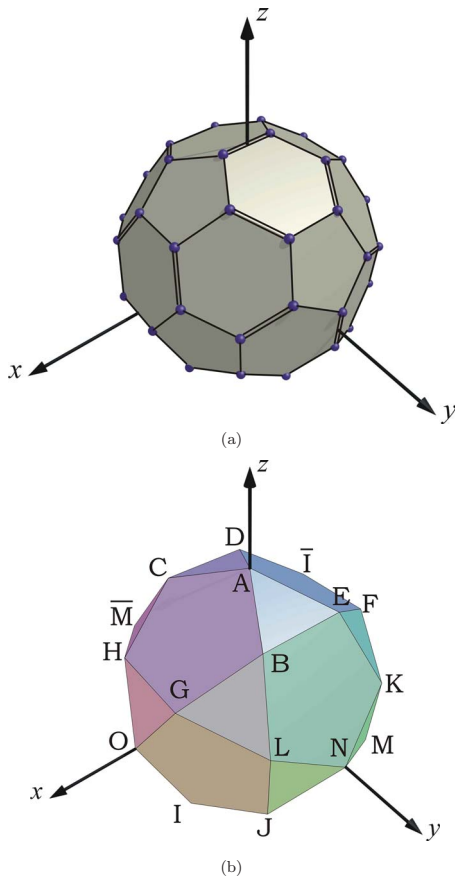


FIG. 1. (Color online) (a) Fullerene $C_{60}$ showing the location of the C-C double bonds, the centers of which coincide with the positions of the $D_{2h}$ wells. (b) An icosidodecahedron formed by connecting the points where the axes of the $D_{2h}$ distortions cut the surface of a sphere. The vertices are labeled $A, B, C, \ldots, O$, as used in Table I.

$$a_i = \boldsymbol{x}_1^{\mathsf{T}} \mathcal{H}'_{int}(Q_j \mapsto \delta_{ij}) \boldsymbol{x}_1 \tag{14}$$

(where $\delta_{ij}$ is the Kronecker $\delta$ function). The outcome of this procedure is that the minimum is attained when

$$a_\theta = A_1 \cos\beta + A_2 \sin\beta,$$

$$a_\epsilon = A_3 \cos\beta + A_4 \sin\beta,$$

$$a_x = a_y = a_z = 0, \tag{15}$$

where

$$A_1 = \frac{\sqrt{10}}{20}(s_1 - s_2)[\sqrt{3}(s_1 + s_2) + 2s_3],$$

$$A_2 = -\frac{\sqrt{3}}{15}A_3 + \frac{2\sqrt{6}}{15}[2(s_1 - s_2)^2 - 1],$$

$$A_3 = -\frac{\sqrt{2}}{4}[s_1^2 + s_2^2 + 2\sqrt{3}s_3(s_1 + s_2)],$$

$$A_4 = -\sqrt{3}A_1. \tag{16}$$

Using Eq. (12) and the positions in Eq. (15) we can now find an expression for the energy of the minimum, including Coulomb term splittings, given by

$$E_{\min} = \lambda_1^{\min} = B_1 + B_2 \sin 2\beta + B_3 \cos 2\beta, \tag{17}$$

where

$$B_1 = \sum_{i=1}^{3} \frac{\mu\omega^2}{V^2}\mathcal{E}_i s_i^2 - \frac{1}{4}\sum_{j=1}^{4} A_j^2,$$

$$B_2 = -\frac{1}{2}(A_1A_2 + A_3A_4),$$

$$B_3 = \frac{1}{4}\sum_{j=1}^{4}(-1)^j A_j^2. \tag{18}$$

The energy given in Eq. (17) depends on the unknown quantities $s_1$ and $s_2$. We determine them by insisting that the molecular response to the term energies should be such that the energy attains its lowest possible value. One immediate conclusion from Eq. (17) is that the system $E_{\min}(s_1, s_2)$ to be minimized does not change if the mixing angle $\beta$ is changed by a factor of $\pm\pi$. Therefore the final minimum energy must be periodic in $\beta$ with a period of $\pi$. This confirms the variation previously found numerically.[15] In addition, $s_1$ and $s_2$ must have the same periodicity as $E_{\min}$. Further consideration shows that if the term energies are such that the $T_1$ and $T_2$ levels remain degenerate (i.e., $\mathcal{E}_{T_1} = \mathcal{E}_{T_2}$), then the minimum energy will be symmetrical about the mixing angle $\beta = 0$. [In this case, a change in sign of $\beta$ causes $E_{min} \mapsto B_1 - B_2 \sin 2\beta + B_3 \cos 2\beta$. However, if we now interchange the variables $s_1$ and $s_2$, we see that $(B_1, B_2, B_3) \mapsto (B_1, -B_2, B_3)$ and so we are again left with the same system to minimize but with the variables $s_1$ and $s_2$ interchanged. The resulting minimum energy will be the same.]

We now seek to find values for $s_1$ and $s_2$ that minimize $E_{\min}$. The resulting pair of equations are highly nonlinear and can only be solved numerically. Three-dimensional plots of Eq. (17) show that these numerical solutions give precisely the required values of $s_1$ and $s_2$ as those obtained by numerical minimizing the lowest-energy eigenvalue of the original Hamiltonian. This justifies the method used here to obtain values for $s_1$ and $s_2$. To progress further, we will simplify matters by confining our attention to the case when the mixing angle $\beta = 0$. This approximation is not too restrictive as $D_{2h}$ minima only occur in the region close to $\beta = 0$, and for the particular case of $C_{60}^{2+}$ ions, it is calculated[1] that the most strongly coupled mode of vibration is the $h_g(1)$ mode which has $\beta \approx 0$. For this case, the equations take the form

$$F(s_1, s_2) - 20\delta'_2 s_1 s_3 = 0,$$

$$F(s_2, s_1) + 20(\delta'_1 - \delta'_2) s_2 s_3 = 0, \tag{19}$$

where

$$\delta_i' = \frac{\delta_i}{V'^2 \hbar\omega} \tag{20}$$

and

$$\delta_1 = \mathcal{E}_{T_2} - \mathcal{E}_{T_1},$$

$$\delta_2 = \mathcal{E}_G - \mathcal{E}_{T_1} \tag{21}$$

are the energies of the $T_2$ and $G$ levels above the $T_1$ level, and where

$$\begin{aligned} F(x,y) = [&4x(7x^2-4) + xy(42x+31y) \\ &+ 14y(y^2-1)]\sqrt{1-x^2-y^2} + \sqrt{3}[3x^2(4x^2-3) \\ &+ x^2y(6x+13y) + xy(7y^2-4) + 2y^2(y^2-1)]. \end{aligned} \tag{22}$$

Once the term energies are specified, Eqs. (19) may be solved to yield the required values of $s_1$ and $s_2$. This also yields the JT energy $E_{JT}$ and position $\boldsymbol{a}$ of the $D_{2h}$ minimum via Eqs. (17) and (15), respectively.

There are, of course, 14 other positions that give rise to equivalent $D_{2h}$ wells with the same minimum energy in the APES. These correspond to the potential wells into which the system may become localized in the limit of infinitely strong coupling. It is a simple matter to generate the positions of the other wells using symmetry operators and the position of the one well obtained above. Similarly, the electronic states for these wells may also be found using the electronic state already derived. Therefore we have complete knowledge of the vibronic states associated with each well. The next step is to use projection operators to form combinations of the $D_{2h}$ wells to account for quantum mechanical tunneling between the wells. This forms the basis of the next section.

## IV. SYMMETRY-ADAPTED STATES AND TUNNELING ENERGIES

The results when the term energies are ignored take particularly simple analytical forms that are useful for making some general observations about the system. We thus cover this case first before investigating the more complicated situation in which the term energies are nonzero.

### A. $\mathcal{H}_{term}=0$

If the term energies due to Coulomb interactions are ignored, the coordinates of the $D_{2h}$ wells and their corresponding electronic states have relatively simple forms, as shown in Table I. This shows that each well has eight nearest neighbors and six next-nearest neighbors. The axes of the distortions corresponding to the generation of each well cut the surface of a sphere at the vertices of an icosidodecahedron, as shown in Fig. 1. It should be noted that when equivalent pictures have been drawn for $D_{5d}$ and $D_{3d}$ distortions,[22] the geometrical separation of the vertices corresponding to the minima represents the division of the wells into nearest and next-nearest neighbors. However, that is not the case with the $D_{2h}$ wells. While wells $B-E$ are nearest neighbors to well $A$ in the figure, wells $J-M$ are not. However, all eight wells are nearest neighbors in the five-dimensional $Q$ space.

For very strong JT coupling, the system is locked into one of these wells and the ion is permanently (statically) distorted. However, the coupling strength will, of course, be finite and so the barriers between wells will also be finite and the ion will be able to pass from one well to another. The nuclear motion accompanying this dynamic JT effect is usually referred to as pseudorotation. On a sufficiently long time scale, pseudorotation averages out the positions of the nuclei leading to an ion having icosahedral symmetry.

The vibronic state appropriate to the transformed picture may be written in the form $|W;0\rangle$, where $|W\rangle$ is the electronic state associated with well $W$ and $|0\rangle$ denotes that all the $h$ oscillators are in their ground state. States $|W';0\rangle$ appropriate to the untransformed picture can then be obtained by multiplying the transformed states by the shift operator $U$ appropriate to that well such that

$$|W';0\rangle = U_W|W;0\rangle. \tag{23}$$

As $U_W$ contains phonon operators, the resultant states are necessarily vibronic.

The ability to delocalize itself over a number of discrete wells has an effect on the energy of the ion. To account for this variation, we can use projection operators to find combinations of the well states that have symmetries corresponding to irreducible representations of the $I_h$ group. Using this technique, the 15 well states are found to produce symmetry-adapted states of $T_{1g}$, $T_{2g}$, $G_g$, and $H_g$ symmetry (see the Appendix), as expected from group theory. It is then a simple matter to find the energies of these symmetry-adapted states (SASs) by forming the appropriate matrix elements. Formulating these matrix elements involves calculating vibronic overlaps between the various wells. For example, the vibronic overlap between nearest-neighbor wells such as $A$ and $B$ is

$$\langle A';0|B';0\rangle = \langle A|B\rangle\langle 0|U_A^\dagger U_B|0\rangle, \tag{24}$$

i.e., a product of electronic and phonon parts, information about which has been included in Table I. Therefore to simplify ensuing calculations, we define the phonon overlap between a well and an adjacent well as

$$S = \langle 0|U_A^\dagger U_B|0\rangle = \exp\left(-\frac{27}{64}V'^2\right). \tag{25}$$

The phonon overlap between next-nearest-neighbor wells, such as $A$ and $F$, is

$$\langle 0|U_A^\dagger U_F|0\rangle = \exp\left(-\frac{27}{32}V'^2\right) = S^2. \tag{26}$$

In terms of these parameters, our calculations yield

$$E_{T_{1g}} = E_{T_{2g}} = E_{T_{Gg}} = \left[\frac{5}{2} - \frac{9}{64}\left(\frac{8+7S}{2+S}\right)V'^2\right]\hbar\omega \tag{27}$$

and

TABLE I. Properties of the 15 minima of $D_{2h}$ symmetry grouped according to their equivalence with respect to minimum $A$. A mixing angle of $\beta=0$ has been assumed and term energies set to zero. The positions correspond to the coordinates $\boldsymbol{a}$ of the minima. The associated (normalized) electronic states are written in terms of their components in the $\{T_{1g},T_{2g},G_g\}$ basis and the golden mean $\phi=\frac{1}{2}(1+\sqrt{5})$. Also shown are the phonon and electronic overlaps between the minima and minimum $A$, where $V'=-V/\sqrt{\mu\hbar\omega^3}$ is a dimensionless linear coupling constant. Each of the minima is at an energy $E=-E_{JT}=-\frac{9}{16}V'^2\hbar\omega$.

| Label | Position | Phonon overlap | Electronic state | Electronic overlap |
|---|---|---|---|---|
| $A$ | $-\frac{3}{4}(0,\sqrt{2},0,0,0)$ | 1 | $\sqrt{\frac{3}{10}}(0,0,1,0,0,1,0,0,0,\frac{2}{\sqrt{3}})$ | 1 |
| $B$ | $-\frac{3}{16}(-\sqrt{6},\sqrt{2},-2\sqrt{3},0,-2\sqrt{3})$ | | $\frac{1}{2}\sqrt{\frac{3}{10}}(\phi^{-1},1,\phi,-\phi,1,-\phi^{-1},-\sqrt{\frac{5}{3}},-\frac{1}{\sqrt{3}},-\sqrt{3},\frac{1}{\sqrt{3}})$ | |
| $C$ | $-\frac{3}{16}(-\sqrt{6},\sqrt{2},2\sqrt{3},0,2\sqrt{3})$ | | $\frac{1}{2}\sqrt{\frac{3}{10}}(\phi^{-1},-1,\phi,-\phi,-1,-\phi^{-1},\sqrt{\frac{5}{3}},-\frac{1}{\sqrt{3}},\sqrt{3},\frac{1}{\sqrt{3}})$ | |
| $D$ | $-\frac{3}{16}(-\sqrt{6},\sqrt{2},2\sqrt{3},0,-2\sqrt{3})$ | | $\frac{1}{2}\sqrt{\frac{3}{10}}(-\phi^{-1},-1,\phi,\phi,-1,-\phi^{-1},-\sqrt{\frac{5}{3}},\frac{1}{\sqrt{3}},\sqrt{3},\frac{1}{\sqrt{3}})$ | |
| $E$ | $-\frac{3}{16}(-\sqrt{6},\sqrt{2},-2\sqrt{3},0,2\sqrt{3})$ | $\exp(-\frac{27}{64}V'^2)$ | $\frac{1}{2}\sqrt{\frac{3}{10}}(-\phi^{-1},1,\phi,\phi,1,-\phi^{-1},\sqrt{\frac{5}{3}},\frac{1}{\sqrt{3}},-\sqrt{3},\frac{1}{\sqrt{3}})$ | $\frac{1}{4}$ |
| $J$ | $-\frac{3}{16}(\sqrt{6},\sqrt{2},0,2\sqrt{3},-2\sqrt{3})$ | | $\frac{1}{2}\sqrt{\frac{3}{10}}(1,\phi,-\phi^{-1},1,-\phi^{-1},\phi,\sqrt{\frac{5}{3}},-\sqrt{3},\frac{1}{\sqrt{3}},\frac{1}{\sqrt{3}})$ | |
| $K$ | $-\frac{3}{16}(\sqrt{6},\sqrt{2},0,2\sqrt{3},2\sqrt{3})$ | | $\frac{1}{2}\sqrt{\frac{3}{10}}(1,-\phi,-\phi^{-1},1,\phi^{-1},\phi,-\sqrt{\frac{5}{3}},-\sqrt{3},-\frac{1}{\sqrt{3}},\frac{1}{\sqrt{3}})$ | |
| $L$ | $-\frac{3}{16}(\sqrt{6},\sqrt{2},0,-2\sqrt{3},-2\sqrt{3})$ | | $\frac{1}{2}\sqrt{\frac{3}{10}}(-1,-\phi,-\phi^{-1},-1,\phi^{-1},\phi,\sqrt{\frac{5}{3}},\sqrt{3},-\frac{1}{\sqrt{3}},\frac{1}{\sqrt{3}})$ | |
| $M$ | $-\frac{3}{16}(\sqrt{6},\sqrt{2},0,-2\sqrt{3},2\sqrt{3})$ | | $\frac{1}{2}\sqrt{\frac{3}{10}}(-1,\phi,-\phi^{-1},-1,-\phi^{-1},\phi,-\sqrt{\frac{5}{3}},\sqrt{3},\frac{1}{\sqrt{3}},\frac{1}{\sqrt{3}})$ | |
| $F$ | $-\frac{3}{8}(0,-\sqrt{2},-\sqrt{3},\sqrt{3},0)$ | | $\frac{1}{2}\sqrt{\frac{3}{10}}(\phi,-\phi^{-1},-1,-\phi^{-1},\phi,-1,-\sqrt{\frac{5}{3}},\frac{1}{\sqrt{3}},\frac{1}{\sqrt{3}},\sqrt{3})$ | |
| $G$ | $-\frac{3}{8}(0,-\sqrt{2},-\sqrt{3},-\sqrt{3},0)$ | | $\frac{1}{2}\sqrt{\frac{3}{10}}(-\phi,-\phi^{-1},-1,\phi^{-1},\phi,-1,\sqrt{\frac{5}{3}},-\frac{1}{\sqrt{3}},\frac{1}{\sqrt{3}},\sqrt{3})$ | |
| $H$ | $-\frac{3}{8}(0,-\sqrt{2},\sqrt{3},-\sqrt{3},0)$ | $\exp(-\frac{27}{32}V'^2)$ | $\frac{1}{2}\sqrt{\frac{3}{10}}(-\phi,\phi^{-1},-1,\phi^{-1},-\phi,-1,-\sqrt{\frac{5}{3}},-\frac{1}{\sqrt{3}},-\frac{1}{\sqrt{3}},\sqrt{3})$ | 0 |
| $I$ | $-\frac{3}{8}(0,-\sqrt{2},\sqrt{3},\sqrt{3},0)$ | | $\frac{1}{2}\sqrt{\frac{3}{10}}(\phi,\phi^{-1},-1,-\phi^{-1},-\phi,-1,\sqrt{\frac{5}{3}},\frac{1}{\sqrt{3}},-\frac{1}{\sqrt{3}},\sqrt{3})$ | |
| $N$ | $-\frac{3}{8}(\sqrt{6},-\sqrt{2},0,0,0)$ | | $\sqrt{\frac{3}{10}}(0,1,0,0,1,0,0,0,\frac{2}{\sqrt{3}},0)$ | |
| $O$ | $-\frac{3}{8}(-\sqrt{6},-\sqrt{2},0,0,0)$ | | $\sqrt{\frac{3}{10}}(1,0,0,1,0,0,0,\frac{2}{\sqrt{3}},0,0)$ | |

$$E_{H_g}=\left[\frac{5}{2}-\frac{9}{64}\left(\frac{4-7S}{1-S}\right)V'^2\right]\hbar\omega \tag{28}$$

for the energies of the SASs. There are no terms involving $S^2$ in these results because the electronic overlap between next-nearest-neighbor wells is zero. In these expressions, the $\frac{5}{2}\hbar\omega$ corresponds to the zero-point energies of the five uncoupled harmonic oscillators.

In the limit of infinitely strong vibronic coupling when $V'\to\infty$, the phonon overlap $S\to 0$, and both energies tend to the energy $-E_{\mathrm{JT}}+\frac{5}{2}\hbar\omega$. This is the same as the static JT limit, as is to be expected. Conversely, in the limit of weak vibronic coupling $V'\to 0$, the phonon overlap $S\to 1$, and $E_{T_{1g}}$, etc., tend to the zero-point energy $\frac{5}{2}\hbar\omega$. At the same time, $E_{H_g}\to 7\hbar\omega/2$, showing that this state represents a first excited vibronic state. The variation of the energies of the SASs in across the whole coupling regime is shown in Fig. 2. It should be noted that this figure is a corrected version of a similar plot published in Ref. 17. In that work, the abscissae in Fig. 3 need to be scaled by a factor of $\sqrt{2}$ to make the figures consistent with the definition of the linear coupling constant given in that and the current works.

It is interesting to note that the $T_{1g}$, $T_{2g}$, and $G_g$ states are all degenerate irrespective of the strength of the JT coupling, and that they collectively form a ten fold degenerate vibronic ground state. The first excited vibronic state is the fivefold

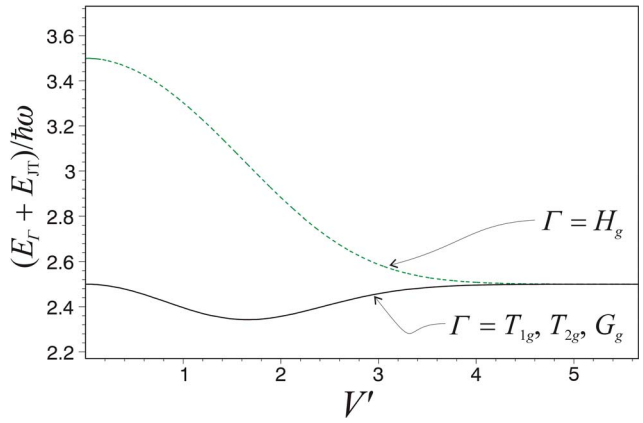


FIG. 2. (Color online) Energies of the symmetry-adapted states when $\mathcal{H}'_{term}=0$. The energies are given relative to $-E_{\mathrm{JT}}$, where $E_{\mathrm{JT}}=9V'^2\hbar\omega/16$.

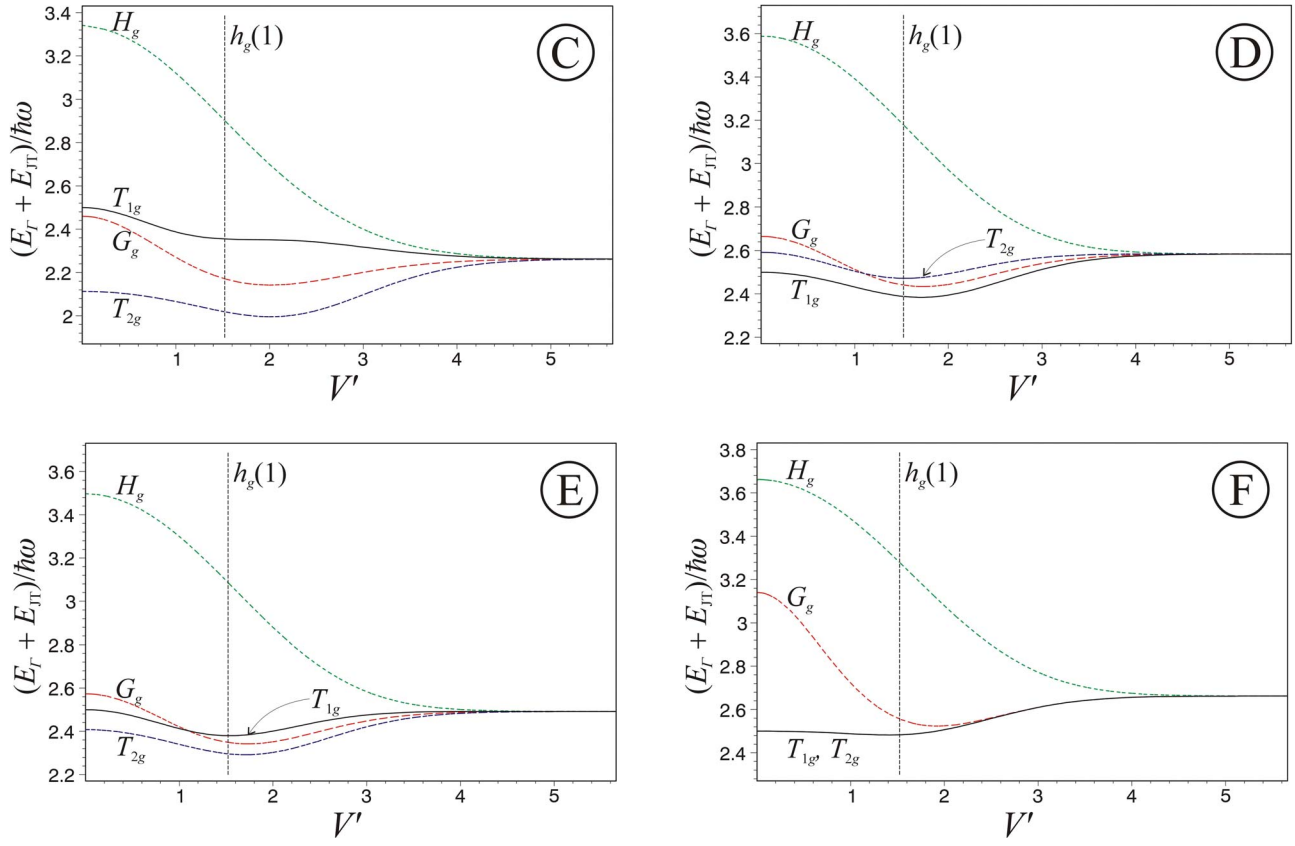


FIG. 3. (Color online) Energies of the symmetry-adapted states in the presence of the term energies as calculated by different authors. The graphs are labeled according to the cases defined in Table II. Case C: Plakhutin *et al.* (Ref. 12) ($\delta_1=-29$, $\delta_2=-3$ meV); Case D: Wierzbowska *et al.* (Ref. 13) ($\delta_1=6.9$, $\delta_2=12.4$ meV); Case E: Wierzbowska *et al.* (Ref. 13) (alternative interpretation, $\delta_1=-6.9$, $\delta_2=5.5$ meV); Case F: Lüders *et al.* (Ref. 4) ($\delta_1=0$, $\delta_2=48$ meV). The dashed vertical line represents the value $V'=1.52$ appropriate to the $h_g(1)$ mode of vibration of $C_{60}$.

degenerate $H_g$ SAS. Any observable differences in energy between the $T_{1g}$, $T_{2g}$, and $G_g$ levels therefore must be due to other mechanisms, e.g., Coulomb interactions, and not the JT effect.

### B. Nonzero term energies

The procedure used in Sec. IV A can be repeated with term energy differences $\delta_1'$ and $\delta_1'$ adopting nonzero values. For a given pair of differences, one must first solve the coupled system in Eq. (19) to find the required values of $s_1$ and $s_2$ which give us the form of the electronic state for our initial well (well $A$). At this stage, caution must be taken to ensure that the term energies have not affected the APES to such an extent that the minima are no longer of $D_{2h}$ symmetry. As discussed in a previous paper,[15] it is possible that minima could be obtained for this system having $D_{2h}$, $C_{2h}$, $D_{5d}$ or $D_{3d}$ symmetries, depending on the mixing angle and term energies. Hence it is essential to check that minima of $D_{2h}$ symmetry are present before using the theory presented here.

In what follows, we use the results of Ref. 15 to restrict ourselves to cases which do indeed involve $D_{2h}$ minima. In order to use our method, we need to choose values for the term energies and so we adopt here values that are specifically aimed at describing the $C_{60}^{2+}$ ion. This, in itself, requires certain approximations to be adopted. First, we assume that the system may be approximated as a single-mode coupling problem involving the $h_g(1)$ normal mode of vibration only (taken to have the experimentally observed frequency,[23] $\hbar\omega \sim 272\ \mathrm{cm}^{-1}$). The justification for this lies in recent DFT calculations[1] which indicate that the $h_g(1)$ normal mode is, by far, the most strongly coupled mode of vibration, having a dimensionless linear coupling parameter of $V'\simeq 1.52$ (the other $h_g$ modes have $V'\lesssim 0.61$ and the $g_g$ modes have $V'\lesssim 0.40$). The calculations of Ref. 1 also indicate that the $h_g(1)$ mode has a mixing angle of $\beta\approx 0$, which makes the mode an ideal candidate for the treatment developed here.

Next, we need to decide on the term energies appropriate to the $C_{60}^{2+}$ cation. Unfortunately, there seems to be several calculations[4,9,12,13] of these parameters for the $C_{60}^{2+}$ ion, none of which are in agreement with the others (see Table II). To overcome this uncertainty, we shall consider each of these possible sets of term energies, except for those calculated by Nikolaev and Michel.[9] This latter work is ignored here for three reasons. First, our previous results indicate that their calculated term energies give rise to minima of $D_{3d}$ symmetry and is therefore not amenable to the theory used here. The second reason is that their calculations indicate that the $C_{60}^{2+}$ anion has a high-spin ground state, in contrast to

TABLE II. Calculated term energy differences taken from the literature. The fourth column gives the symmetry of the minima occurring for a $C_{60}^{2+}$ cation subjected to that particular pattern of term energies (Ref. 15). Case *A* simply labels a hypothetical case in which all terms are degenerate. This is not expected apply to $C_{60}^{2+}$ ions.

| Label | $\delta_1$ (meV) | $\delta_2$ (meV) | Symmetry | Ref. |
|---|---|---|---|---|
| *A* | 0 | 0 | $D_{2h}$ | |
| *B* | 29 | 26 | $D_{3d}$ | 9 |
| *C* | −29 | −3 | $D_{2h}$ | 12 |
| *D* | 6.9 | 12.4 | $D_{2h}$ | 13[a] |
| *E* | −6.9 | 5.5 | $D_{2h}$ | 13[a] |
| *F* | 0 | 48 | $D_{2h}$ | 4 |

[a]These authors cannot distinguish the identity of their triply degenerate states: *D* has $T_{1g}$ lower in energy than $T_{2g}$; *E* has the opposite ordering.

evidence based on EPR measurements reported by Reed and Bolskar[24] which suggest that this anion has a low-spin ground state (and is thus diamagnetic). This therefore casts some doubt upon their results in general. Third, these workers have themselves recently revisited the problem, making more sophisticated calculations, and obtained term energies that differ considerably from their original results.[25]

For each of the calculated sets of term energies *C*–*F*, the energies of the resulting SASs, assuming the presence of $D_{2h}$ minima, can be found using the procedure used in the absence of Coulomb interactions (Sec. IV A). As for that case, we present the resulting energies graphically as a function of the dimensionless linear coupling parameter in Fig. 3. In these graphs, we have marked with a broken vertical line the linear coupling strength appropriate to the $h_g(1)$ vibrational mode of $C_{60}$. This line therefore marks the pattern of energies that should approximate those in the $C_{60}^{2+}$ ion, assuming that the Coulomb interactions have been correctly accounted for. The figures show, unsurprisingly, that the order and energy of the vibronic levels depends on the Coulomb interactions present in the ion. Therefore experimental observation of these energy levels should permit extraction of numerical values for the Coulomb energies in $C_{60}^{2+}$, which may then be compared with the various calculated values.

The graphs in Fig. 3 give an overall impression of the effect of varying the linear vibronic coupling parameter on the vibronic energy levels occurring in $C_{60}^{2+}$. At the calculated coupling strength for the $h_g(1)$ mode, the splittings between the terms due to Coulomb interactions seem somewhat subdued compared to when JT interaction is absent. This is especially true in Fig. 3(F). At this point we must re-emphasize that these graphs are based on a model in which the $C_{60}^{2+}$ ion has minima in its APES of $D_{2h}$ symmetry. Therefore the graphs will not give a true picture if minima of a different symmetry are formed. In particular, in the limit as $V_1' \to 0$ it is clear that the Coulomb interactions will become increasingly more important than the JT interactions. It was shown in an earlier work[15] that this results in a symmetry change. Thus the graphs become invalid for small $V_1'$. However, Ref. 15 also showed that for the $h_g(1)$ mode, the minima in the APES are, in fact, of $D_{2h}$ symmetry for each of the cases *C*–*D* shown in Fig. 3. Therefore we can immediately accept the validity of the graphs in Fig. 3 for the range where $V_1' \gtrsim 1.5$. The graphs in the regime where $0 < V_1' \lesssim 1.5$ may be partially valid. For example, in Fig. 3(D), $D_{2h}$ symmetry persists down to $V_1' \simeq 0.7$. This complication is unimportant in the present context as the calculated coupling strengths in $C_{60}^{2+}$ point towards $D_{2h}$ minima and so we should be dealing with those parts of the graphs wherein the theory does apply.

## V. SUMMARY AND CONCLUSIONS

Previous studies have suggested that the minima in the lowest APES of $C_{60}^{2+}$ are of $D_{2h}$ symmetry.[10,11,15] In this paper, an effective- or single-mode model has been developed for the ion that is based upon the veracity of this prediction. Our calculations have utilized calculated coupling constants[1] because, to the best of our knowledge, there are no experimental values currently available for these quantities. If such data become available, then our calculations here will readily show the results that will be obtained if $D_{2h}$ minima are present. If one of the other possible symmetries that the ion may adopt ($D_{5d}$, $D_{3d}$, and $C_{2h}$) dominates, then it would be necessary to perform a similar procedure to that outlined here but for that different symmetry.

By assuming minima of a particular symmetry, expressions for the vibronic states associated with ions localized within the wells have been formulated and used to create symmetry-adapted states, which give a good description of the ion in the presence of a dynamic JT effect. We have further used these states to calculate term energies and presented the results graphically (Figs. 2 and 3) for a range of vibronic coupling strengths.

Coulomb interactions between the holes in $C_{60}^{2+}$ give rise to energy differences between terms, even in the absence of JT interaction. Unfortunately, the extent of these Coulomb interactions are not accurately known. Therefore we have assessed each of the sets of calculated term energies available in the literature to provide a graphical representation of the term energy differences that are to be expected in the ion if JT interactions are included.

The overall indication is that, at the value of the coupling parameter pertinent to the dominant $h_g(1)$ mode of $C_{60}^{2+}$, the residual effects of Coulomb interactions produce significant, but diminished, splittings between the ground $T_1$, $T_2$, and *G* states. Again, these findings will be greatly enhanced if improved calculations, or better still, experimental values, of the Coulomb energies become available. Nevertheless, the current calculations indicate that experimental observation of these splittings will give a useful insight into the strength of both the Jahn-Teller and Coulomb interactions in $C_{60}^{2+}$ ions.

## ACKNOWLEDGMENTS

We thank A. V. Nikolaev for supplying a copy of recent term energy calculations. We are also grateful to EPSRC for providing funds for this work.

## APPENDIX: SYMMETRY-ADAPTED STATES ARISING FROM THE $D_{2h}$ WELLS

In order to simplify the expressions in this Appendix, we denote the vibronic state $|W';0\rangle$ appropriate to well $W$ by $\mathcal{W}$, where the wells are labeled as in Table I. Using projection operators, the symmetry-adapted states are found to be

$$|T_{1g}x\rangle = \frac{N_1}{2\sqrt{5}}[\phi^{-1}(\mathcal{B}+\mathcal{C}-\mathcal{D}-\mathcal{E})+\phi(\mathcal{F}-\mathcal{G}-\mathcal{H}+\mathcal{I})+\mathcal{J}+\mathcal{K}-\mathcal{L}-\mathcal{M}+2\mathcal{O}],$$

$$|T_{1g}y\rangle = \frac{N_1}{2\sqrt{5}}[\mathcal{B}-\mathcal{C}-\mathcal{D}+\mathcal{E}-\phi^{-1}(\mathcal{F}+\mathcal{G}-\mathcal{H}-\mathcal{I})+\phi(\mathcal{J}-\mathcal{K}-\mathcal{L}+\mathcal{M})+2\mathcal{N}],$$

$$|T_{1g}z\rangle = \frac{N_1}{2\sqrt{5}}[2\mathcal{A}+\phi(\mathcal{B}+\mathcal{C}+\mathcal{D}+\mathcal{E})-(\mathcal{F}+\mathcal{G}+\mathcal{H}+\mathcal{I})-\phi^{-1}(\mathcal{J}+\mathcal{K}+\mathcal{L}+\mathcal{M})], \quad \text{(A1)}$$

$$|T_{2g}x\rangle = \frac{N_1}{2\sqrt{5}}[-\phi(\mathcal{B}+\mathcal{C}-\mathcal{D}-\mathcal{E})-\phi^{-1}(\mathcal{F}-\mathcal{G}-\mathcal{H}+\mathcal{I})+\mathcal{J}+\mathcal{K}-\mathcal{L}-\mathcal{M}+2\mathcal{O}],$$

$$|T_{2g}y\rangle = \frac{N_1}{2\sqrt{5}}[\mathcal{B}-\mathcal{C}-\mathcal{D}+\mathcal{E}+\phi(\mathcal{F}+\mathcal{G}-\mathcal{H}-\mathcal{I})-\phi^{-1}(\mathcal{J}-\mathcal{K}-\mathcal{L}+\mathcal{M})+2\mathcal{N}],$$

$$|T_{2g}z\rangle = \frac{N_1}{2\sqrt{5}}[2\mathcal{A}-\phi^{-1}(\mathcal{B}+\mathcal{C}+\mathcal{D}+\mathcal{E})-(\mathcal{F}+\mathcal{G}+\mathcal{H}+\mathcal{I})+\phi(\mathcal{J}+\mathcal{K}+\mathcal{L}+\mathcal{M})], \quad \text{(A2)}$$

$$|G_g a\rangle = \frac{N_1}{2\sqrt{3}}[-\mathcal{B}+\mathcal{C}-\mathcal{D}+\mathcal{E}-\mathcal{F}+\mathcal{G}-\mathcal{H}+\mathcal{I}+\mathcal{J}-\mathcal{K}+\mathcal{L}-\mathcal{M}],$$

$$|G_g x\rangle = \frac{N_1}{2\sqrt{15}}[-\mathcal{B}-\mathcal{C}+\mathcal{D}+\mathcal{E}+\mathcal{F}-\mathcal{G}-\mathcal{H}+\mathcal{I}-3(\mathcal{J}+\mathcal{K}-\mathcal{L}-\mathcal{M})+4\mathcal{O}],$$

$$|G_g y\rangle = \frac{N_1}{2\sqrt{15}}[-3(\mathcal{B}-\mathcal{C}-\mathcal{D}+\mathcal{E})+\mathcal{F}+\mathcal{G}-\mathcal{H}-\mathcal{I}+\mathcal{J}-\mathcal{K}-\mathcal{L}+\mathcal{M}+4\mathcal{N}],$$

$$|G_g z\rangle = \frac{N_1}{2\sqrt{15}}[4\mathcal{A}+\mathcal{B}+\mathcal{C}+\mathcal{D}+\mathcal{E}+3(\mathcal{F}+\mathcal{G}+\mathcal{H}+\mathcal{I})+\mathcal{J}+\mathcal{K}+\mathcal{L}+\mathcal{M}], \quad \text{(A3)}$$

$$|H_g\theta\rangle = \frac{N_2}{2\sqrt{6}}[\mathcal{B}-\mathcal{C}+\mathcal{D}-\mathcal{E}-2(\mathcal{F}-\mathcal{G}+\mathcal{H}-\mathcal{I})-\mathcal{J}+\mathcal{K}-\mathcal{L}+\mathcal{M}],$$

$$|H_g\epsilon\rangle = \frac{N_2}{2\sqrt{2}}[\mathcal{B}-\mathcal{C}+\mathcal{D}-\mathcal{E}+\mathcal{J}-\mathcal{K}+\mathcal{L}-\mathcal{M}],$$

$$|H_g x\rangle = \frac{N_2}{2\sqrt{3}}[\mathcal{B}+\mathcal{C}-\mathcal{D}-\mathcal{E}-\mathcal{F}+\mathcal{G}+\mathcal{H}-\mathcal{I}+2\mathcal{O}],$$

$$|H_g y\rangle = \frac{N_2}{2\sqrt{3}}[-\mathcal{F}-\mathcal{G}+\mathcal{H}+\mathcal{I}-\mathcal{J}+\mathcal{K}+\mathcal{L}-\mathcal{M}+2\mathcal{N}],$$

$$|H_g z\rangle = \frac{N_2}{2\sqrt{3}}[2\mathcal{A}-\mathcal{B}-\mathcal{C}-\mathcal{D}-\mathcal{E}-\mathcal{J}-\mathcal{K}-\mathcal{L}-\mathcal{M}]. \quad \text{(A4)}$$

In these expressions, $N_1$ and $N_2$ are normalization constants given by

$$N_1 = \left(1+\frac{1}{2}S\right)^{-1/2},$$

$$N_2 = (1-S)^{-1/2}, \quad \text{(A5)}$$

where $S$ is the phonon overlap given in Eq. (25).

*Present address: Department of Physics, King Abdulaziz University, Jeddah, Saudi Arabia.
†colin.bates@nottingham.ac.uk
‡Author to whom correspondence should be addressed. janette.dunn@nottingham.ac.uk; URL: http://www.nottingham.ac.uk/~ppzjld

[1] N. Manini, A. Dal Corso, M. Fabrizio, and E. Tosatti, Philos. Mag. B **81**, 793 (2001).
[2] Y.-S. Yi, L. Tian, C.-L. Wang, Z.-B. Su, and L. Yu, Physica C **282-287**, 1927 (1997).
[3] S. E. Canton, A. J. Yencha, E. Kukk, J. D. Bozek, M. C. A. Lopes, G. Snell, and N. Berrah, Phys. Rev. Lett. **89**, 045502 (2002).
[4] M. Lüders, A. Bordoni, N. Manini, A. Dal Corsa, M. Fabrizio, and E. Tosatti, Philos. Mag. B **82**, 1611 (2002).
[5] M. C. M. O'Brien, Phys. Rev. B **53**, 3775 (1996).
[6] A. Ceulemans and P. W. Fowler, J. Chem. Phys. **93**, 1221 (1990).
[7] C. P. Moate, M. C. M. O'Brien, J. L. Dunn, C. A. Bates, Y. M. Liu, and V. Z. Polinger, Phys. Rev. Lett. **77**, 4362 (1996).
[8] N. Manini, Phys. Rev. A **71**, 032503 (2005).
[9] A. V. Nikolaev and K. H. Michel, J. Chem. Phys. **117**, 4761 (2002).
[10] M. Lüders, N. Manini, P. Gattari, and E. Tosatti, Eur. Phys. J. B

**35**, 57 (2003).
[11] M. Lüders and N. Manini, Adv. Quantum Chem. **44**, 289 (2003).
[12] B. N. Plakhutin, J. Chem. Phys. **119**, 11429 (2003).
[13] M. Wierzbowska, M. Luders, and E. Tosatti, J. Phys. B **37**, 2685 (2004).
[14] P. W. Fowler and A. Ceulemans, Mol. Phys. **54**, 767 (1985).
[15] I. D. Hands, J. L. Dunn, W. A. Diery, and C. A. Bates, Phys. Rev. B **73**, 115435 (2006).
[16] M. Saito, Phys. Rev. B **65**, 220508(R) (2002).
[17] I. D. Hands, W. A. Diery, J. L. Dunn, and C. A. Bates, J. Mol. Struct. **838**, 66 (2007).
[18] W. A. Diery, Ph.D. thesis, University of Nottingham, Nottingham, 2005.
[19] W. A. Diery, J. L. Dunn, and C. A. Bates, Fullerenes, Nanotubes, Carbon Nanostruct. **14**, 573 (2006).
[20] N. Manini and P. De Los Rios, Phys. Rev. B **62**, 29 (2000).
[21] C. A. Bates, J. L. Dunn, and E. Sigmund, J. Phys. C **20**, 1965 (1987).
[22] J. L. Dunn and C. A. Bates, Phys. Rev. B **52**, 5996 (1995).
[23] T. J. Dennis, J. P. Hare, H. W. Kroto, R. Taylor, and D. R. M. Walton, Spectrochim. Acta, Part A **47**, 1289 (1991).
[24] C. A. Reed and R. D. Bolskar, Chem. Rev. (Washington, D.C.) **100**, 1075 (2000), see Sec. C, p. 1106.
[25] A. V. Nikolaev (private communication).